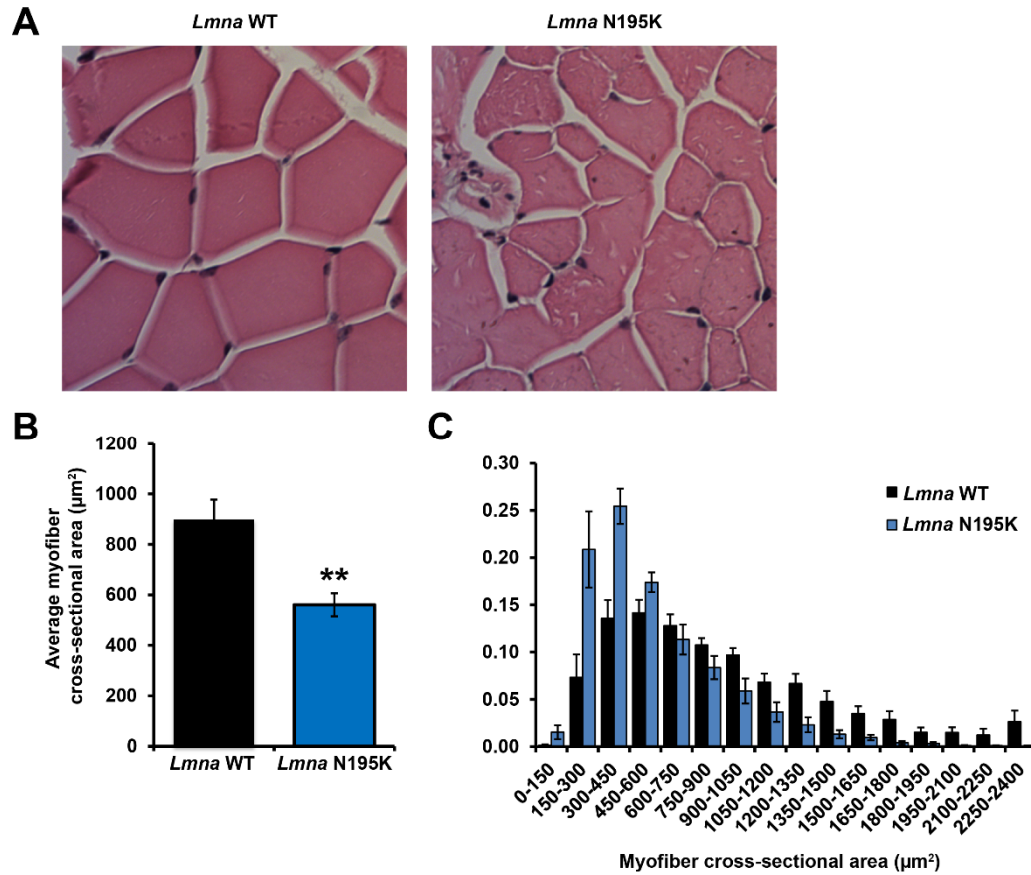
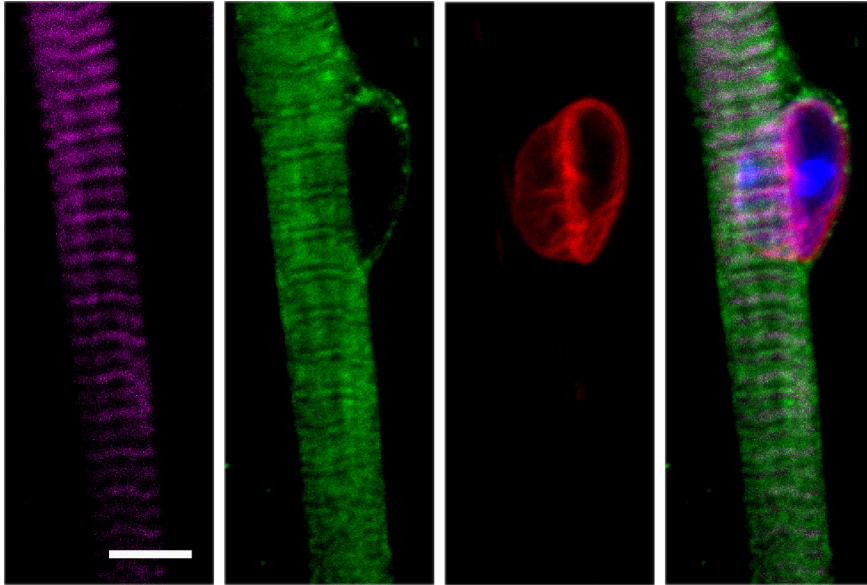


SUPPLEMENTAL FIGURES



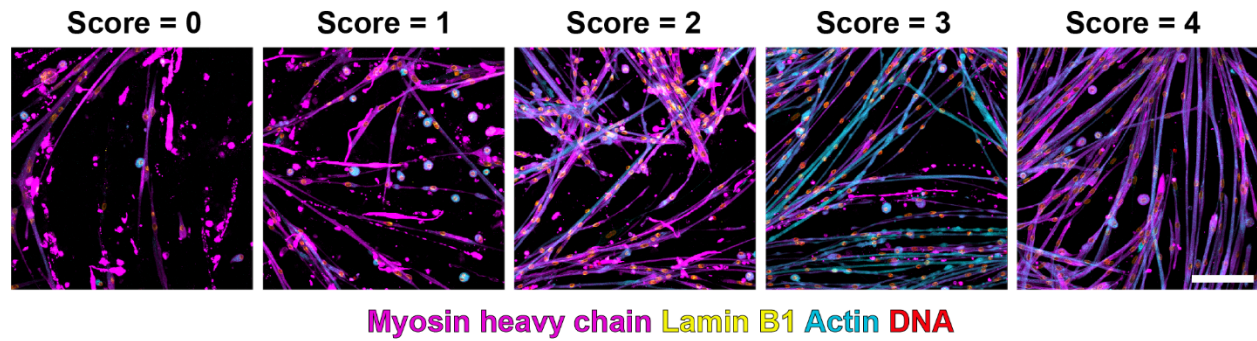
Supplemental Figure 1. *Lmna* N195K mice develop muscular dystrophy. (A) Representative H & E images of skeletal muscle from *Lmna* WT and *Lmna* N195K animal. Scale bar =20 μm . (B) Quantification of the average myofiber cross-sectional area of *Lmna* WT and *Lmna* N195K mice. (C) Relative frequency of myofiber cross-sectional area in *Lmna* WT and *Lmna* N195K mice. $n = 11-12$ animals per genotype.



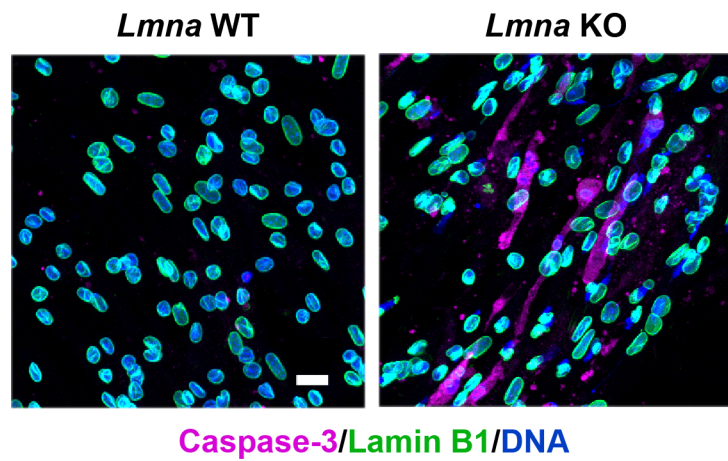
Actin Myosin heavy chain Lamin B1 DNA

Supplemental Figure 2. *In vitro* differentiation results in mature myofibers. Representative image of a striated myofiber containing a peripheral nucleus at day 10 of differentiation. Scale bar = 5 μm .

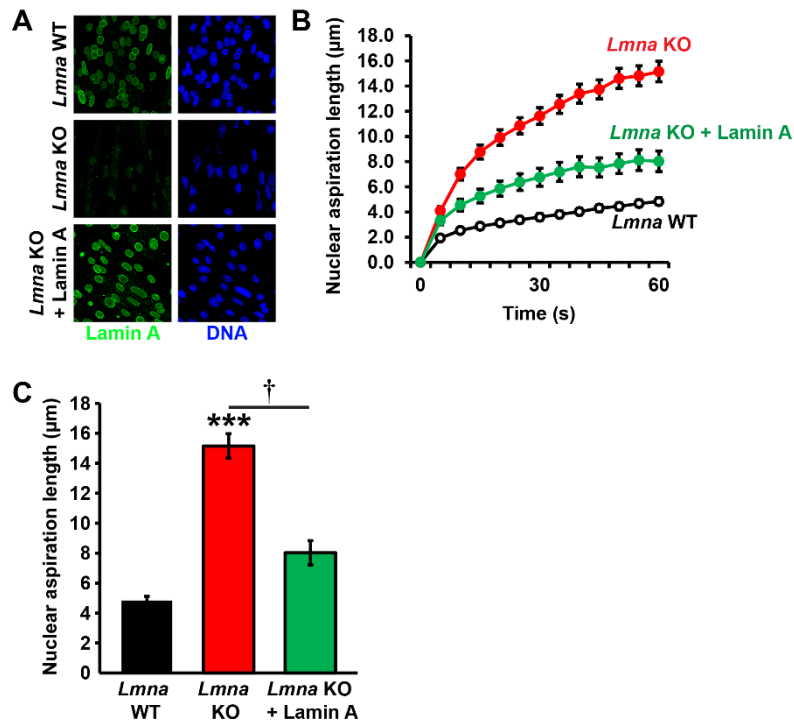
Health score for myofibers



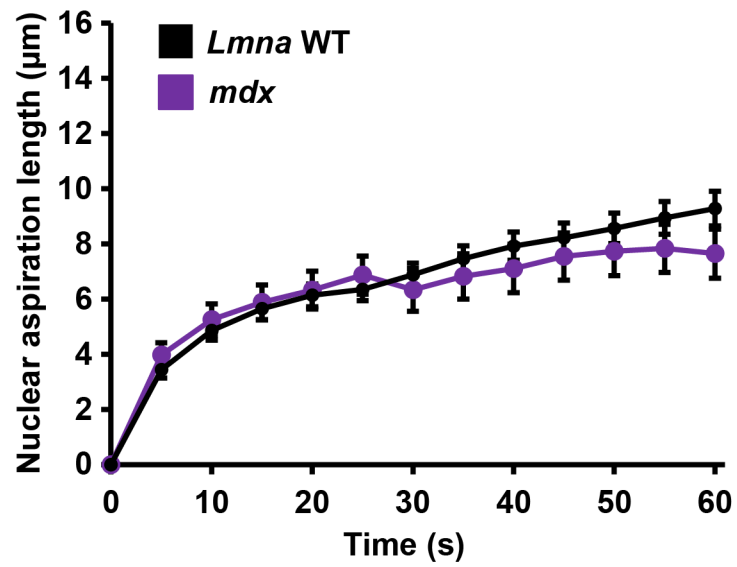
Supplemental Figure 3. Myofiber health scores. Panel of representative images for different myofiber health scores used for quantification of myofiber health. Scale bar = 50 μ m.



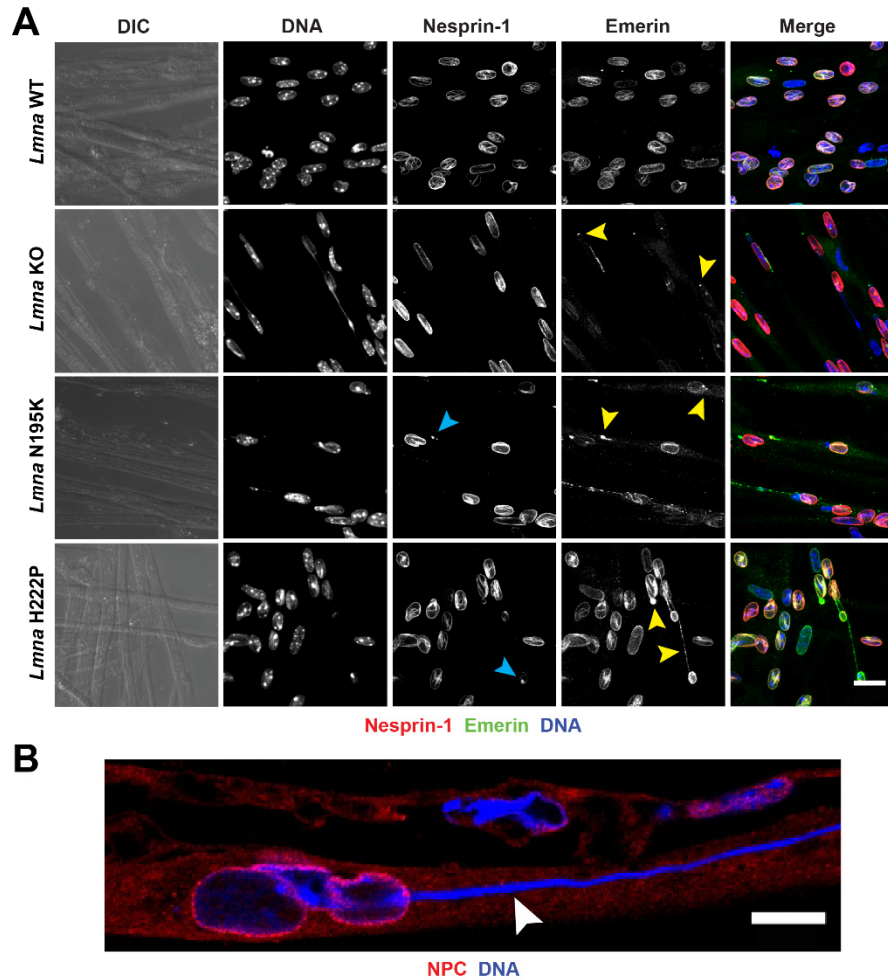
Supplemental Figure 4. *Lmna* mutant myofibers show increased caspase-3 activity. Representative image of immunofluorescence detection of active caspase-3 at day 10 of differentiation. Scale bar = 20 μ m.



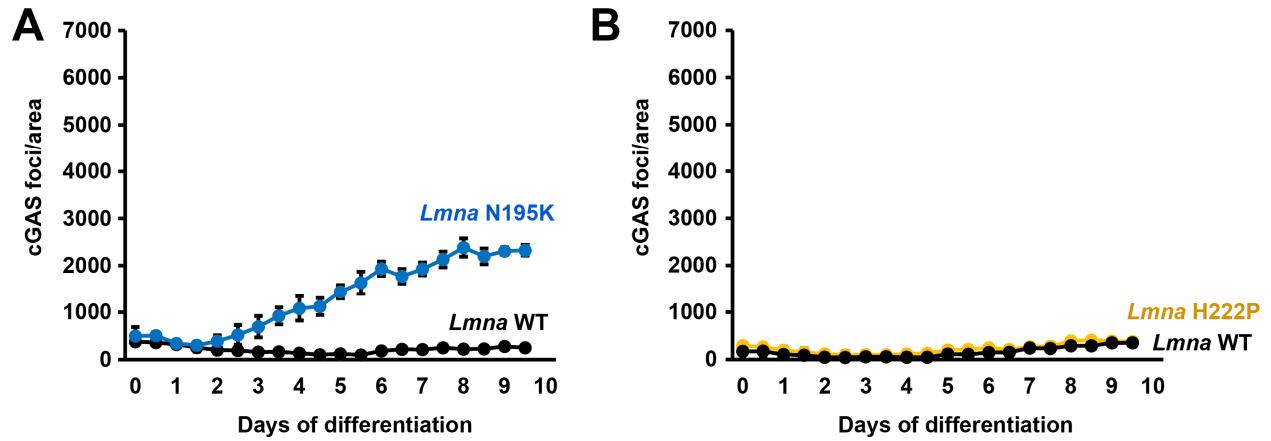
Supplemental Figure 5. Micropipette aspiration analysis of *Lmna* mutant myoblasts and *Lmna* KO myoblasts ectopically expressing lamin A. **(A)** Natural log transformation and plot of the micropipette aspiration data shown in Fig. 2B. The log-log data fits a linear regression model, in which all three *Lmna* mutants were significantly different ($p < 0.001$) from the wild-type controls. The slopes of the log-log data were not significantly different between the samples. A multilevel model including day-to-day variability confirmed that all three *Lmna* mutants were significantly different from the wild-type controls ($p < 0.0001$ for *Lmna* KO and *Lmna* N195K; $p < 0.001$ for *Lmna* H222P), although the statistical significance for the *Lmna* H222P myoblasts was lost when including additional variance components. **(B)** Representative immunofluorescence images of lamin A expression in *Lmna* WT, *Lmna* KO and *Lmna* KO cells ectopically expressing lamin A (*Lmna* KO + lamin A). **(C)** Measurement for nuclear deformation at 5 second intervals for *Lmna* WT, *Lmna* KO, and *Lmna* KO + Lamin A myoblasts during 60 seconds of aspiration. **(D)** Quantification of the nuclear deformation after 60 seconds of aspiration, showing that ectopic expression of lamin A significantly improves nuclear stiffness in *Lmna* KO myoblasts. $n = 41-67$ nuclei per genotype from 3 independent experiments. $n = 62-73$ nuclei per genotype from 3 independent experiments. ***, $p < 0.001$ vs *Lmna* WT cells. †, $p < 0.01$ vs. *Lmna* KO cells.



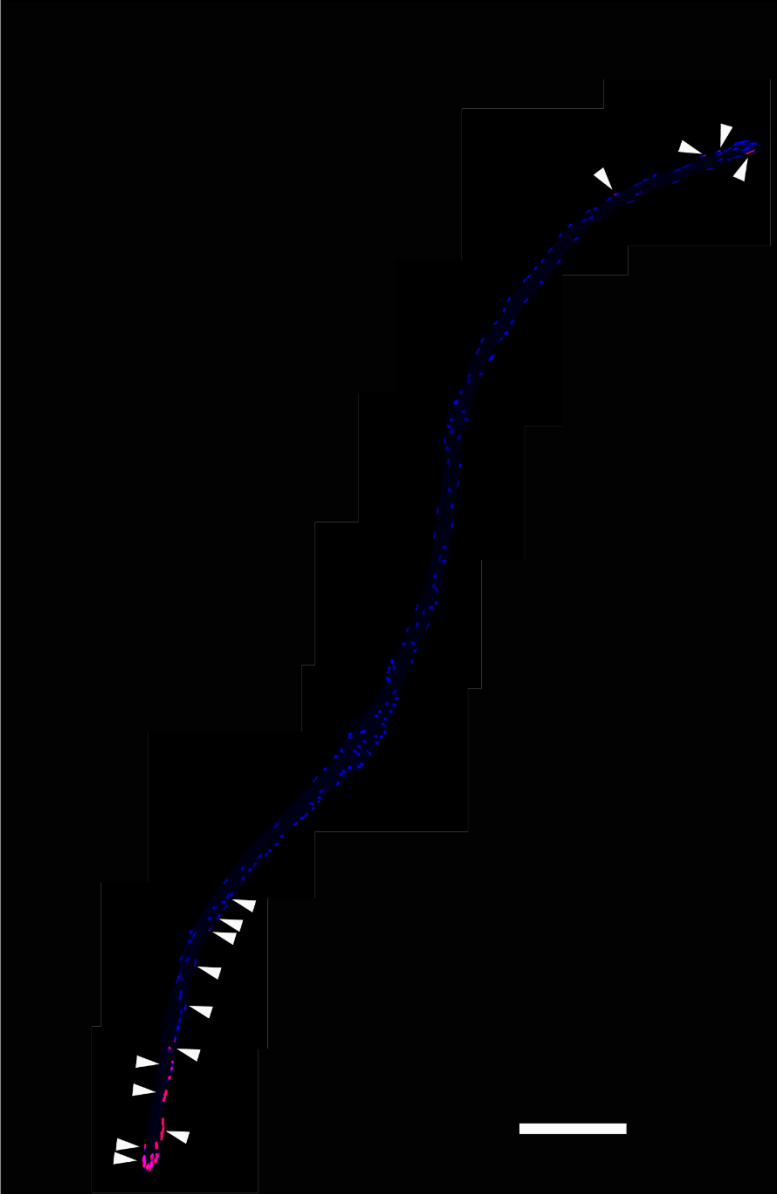
Supplemental Figure 6. *Mdx* myoblasts have normal nuclear stiffness. Measurement for nuclear deformation at 5 second intervals for *Lmna* WT and *mdx* myoblasts during 60 seconds of aspiration. $n = 35-67$ cells per condition.



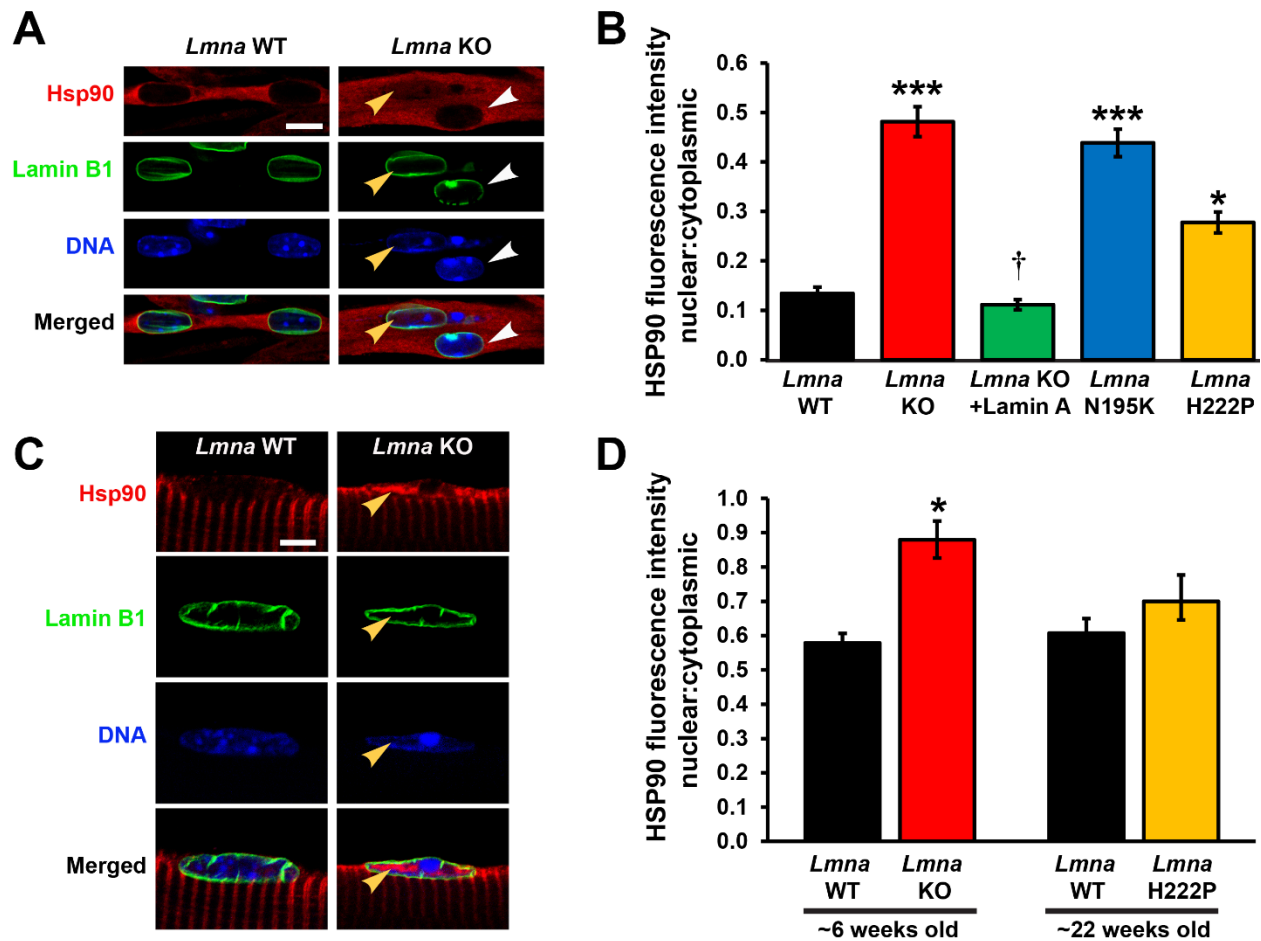
Supplemental Figure 7. Chromatin protrusions are surrounded by nuclear membranes containing emerin, with disturbed localization of nesprin-1 and nuclear pores. **(A)** Representative immunofluorescence images for nesprin-1 and emerin in *Lmna* WT, *Lmna* KO, *Lmna* N195K and *Lmna* H222P myofibers at day 5 of differentiation. Blue and yellow arrows denote chromatin protrusions that are enriched with nesprin-1 and emerin, respectively. Scale bar = 20 μ m. **(B)** Representative image of immunofluorescence detection of nuclear pore complexes (NPC) in *Lmna* KO myofibers at day 10 of differentiation. Scale bar = 10 μ m.



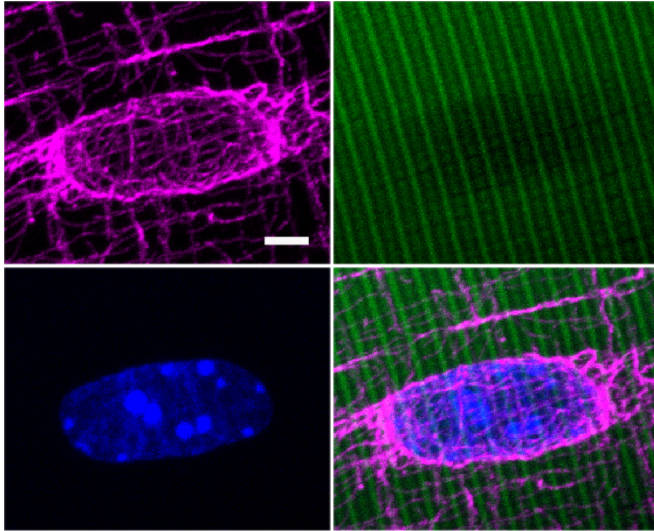
Supplemental Figure 8. Nuclear envelope rupture is increased in *Lmna* N195K myofibers. Quantification of cGAS-mCherry nuclear envelope rupture reporter foci formation during 10 myofiber differentiation in *Lmna* N195K, *Lmna* H222P, and *Lmna* WT cells.



Supplemental Figure 9. Nuclear envelope rupture in *Lmna* KO muscle fibers is increased at myotendinous junctions. Representative image of a single isolated muscle fiber demonstrating the enrichment of cGAS+ nuclei at the myotendinous junctions. Scale bar = 200 μ m.

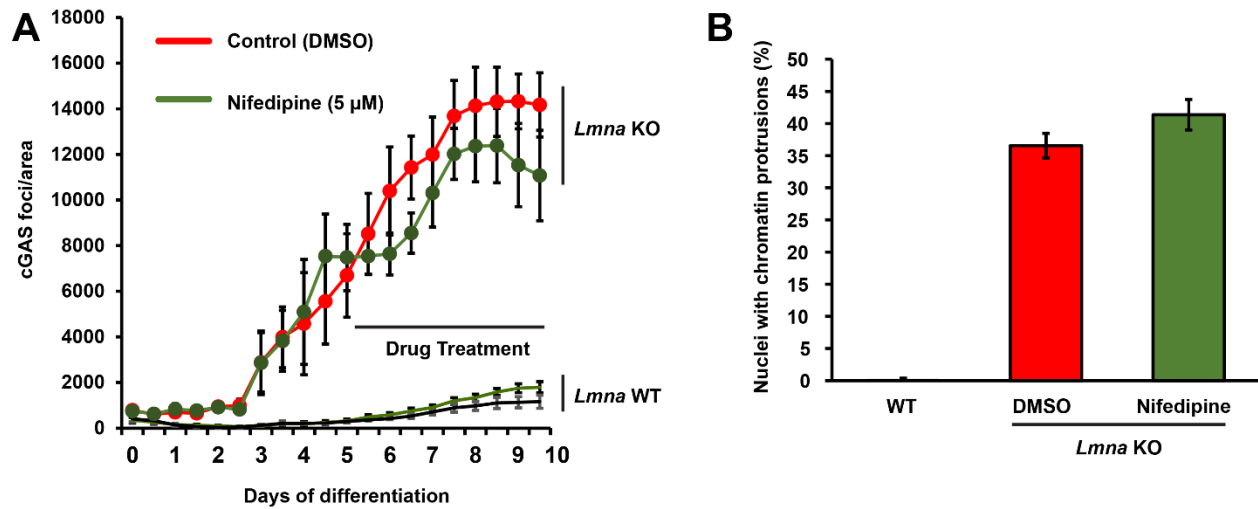


Supplemental Figure 10. *Lmna* mutant myonuclei have increased presence of Hsp90 *in vitro* and *in vivo*. (A) Representative image of nuclear localization of a large cytosolic protein, Hsp90, inside *Lmna* KO nuclei in myofiber differentiated for 10 days. White arrow indicates a nucleus with no observable chromatin defect and little Hsp90 nuclear accumulation, while the yellow arrow marks a nucleus with a chromatin protrusion and increased nuclear Hsp90 accumulation. Scale bar = 10 μ m. (B) Quantification of the fluorescence intensity of nuclear Hsp90 levels for *Lmna* WT, *Lmna* KO, *Lmna* KO + Lamin A, *Lmna* N195K and *Lmna* H222P myofibers *in vitro*. For each nucleus, the nuclear fluorescence intensity was normalized to the cytosolic intensity immediately adjacent to each nucleus. $n = 25-56$ nuclei per genotype from 3 independent experiments. ***, $p < 0.001$ vs. *Lmna* WT ($p < 0.001$). (C) Representative image of Hsp90 nuclear localization in myonuclei from *Lmna* WT and *Lmna* KO mice. Scale bar = 10 μ m. (D) Quantification of the fluorescence intensity of nuclear HSP90 levels for *Lmna* WT, *Lmna* KO, and *Lmna* H222P isolated single fibers. For each nucleus, the nuclear fluorescence intensity was normalized to the cytosolic intensity immediately beside each nucleus $n = 25-56$ nuclei per genotype from 3 independent experiments. ***, $p < 0.001$ vs. *Lmna* WT.

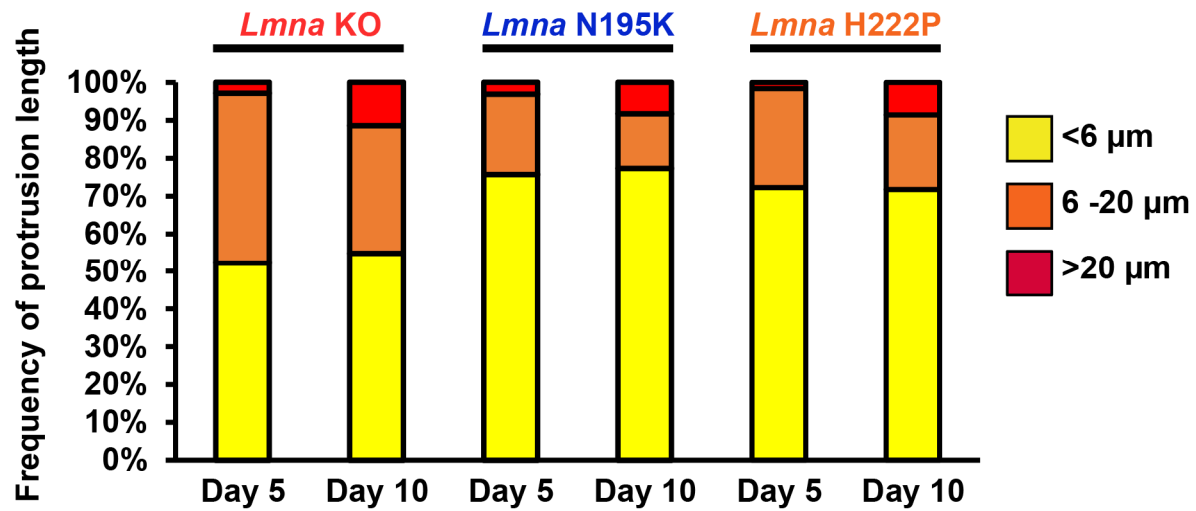


α -Tubulin Actin DNA

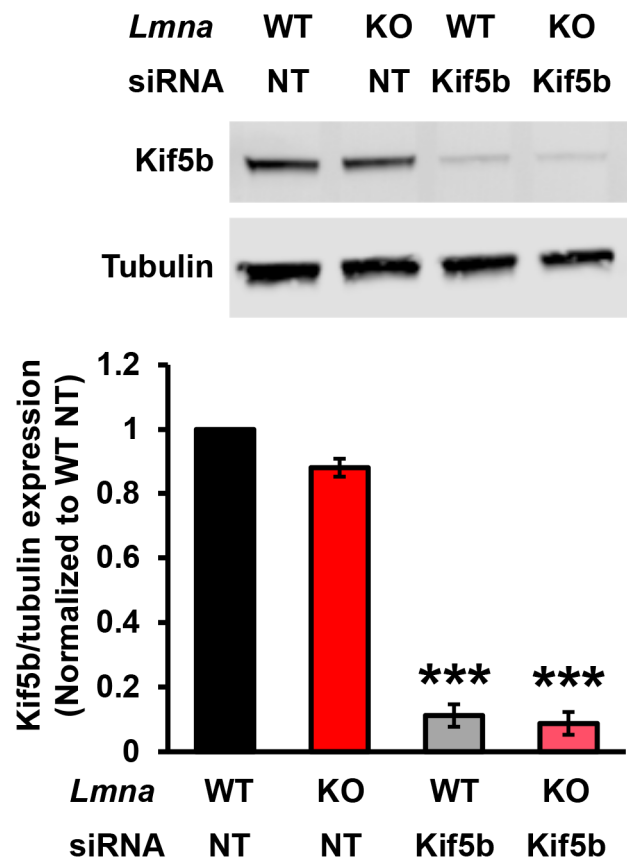
Supplemental Figure 11. Microtubules for cage-like structures around myonuclei. Representative immunofluorescence image of an isolated *Lmna* WT muscle fiber stained for tubulin (magenta), F-actin (green), and DNA (blue), showing characteristic ‘microtubule cage’ around myonucleus. Scale bar = 5 μ m.



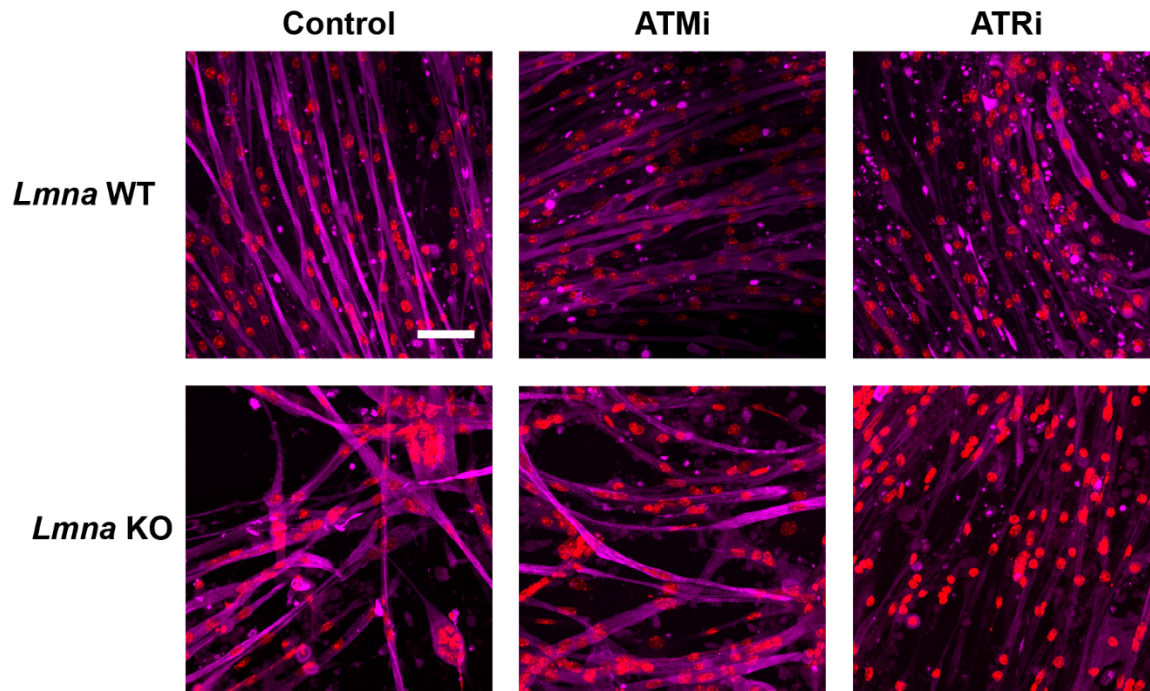
Supplemental Figure 12. Inhibiting myofiber contractility does not prevent nuclear envelope rupture in *Lmna* KO myofibers. (A) Quantification of cGAS-mCherry foci formation during 10 day myofiber differentiation follow treatment with nifedipine (5 μ M), which inhibits contractility, or DMSO vehicle control, starting at day 5 of differentiation. $N = 3$ independent experiments. (B) Quantification of chromatin protrusions at day 7 of differentiation following treatment with nifedipine (5 μ M) or DMSO, starting at day 4. Data generated from $n = 3$ independent experiments in which 27-53 nuclei were analyzed per genotype.



Supplemental Figure 13. Fraction of nuclei with severe chromatin protrusions increased over time in *Lmna* mutant myofibers. Quantification of the relative distribution of chromatin protrusion lengths in *Lmna* KO, *Lmna* N195K and *Lmna* H222P muscle cells at day 5 and day 10 of *in vitro* differentiation.



Supplemental Figure 14. Analysis of Kif5b depletion by siRNA. **(Top)** Western blot for Kif5b in myoblasts treated with a non-target control siRNA (siRNA NT) or siRNA against Kif5b. $n = 3$ independent experiments. **(Bottom)** Corresponding quantification. ***, $p < 0.001$ vs. respective genotype siRNA NT control.



Supplemental Figure 15. ATM and ATR inhibition exacerbates *Lmna* KO myofiber health. Representative images of *Lmna* WT and *Lmna* KO myofibers following treatment with either an ATM inhibitor (KU55933, 5 μ M), ATR inhibitor (VE-821, 5 μ M) or DMSO vehicle control from days 7-14 of differentiation. Scale bar = 50 μ m.

SUPPLEMENTAL MOVIES

Supplemental Movies 1-4. Representative movies of spontaneous contractions in *Lmna* WT, *Lmna* KO, *Lmna* N195K, and *Lmna* H222P myofibers after 10 days of differentiation.

Supplemental Movie 5. Representative movie of micropipette aspiration of *Lmna* WT, *Lmna* KO *Lmna* N195K, and *Lmna* H222P myoblasts.

Supplemental Movie 6. Representative movie of microharpoon manipulation of *Lmna* WT and *Lmna* KO myotubes after day 5 of differentiation.

Supplemental Movie 7. Time-lapse of nuclear envelope rupture during myonuclear spacing at 5 days of differentiation. Note the loss of NLS-GFP from the nucleus is immediately followed by the formation of a cGAS foci at the site of rupture.

Supplemental Movie 8. Representative movie of microharpoon manipulation of *Lmna* KO myotubes after day 5 of differentiation following 24 hour treatment with either 50 nM paclitaxel or DMSO control.

Supplemental Movies 9-10. Representative movies of spontaneous contractions in *Lmna* KO myofibers at 14 days of differentiation following treatment with NU7741 (1 μ M) or DMSO control during 7 to 14 days of differentiation.

Supplemental Tables

Antibody	Cat#	Vendor	Dilution
MyHC	A4.1025	DSHB	1:100
MyHC	MAB4470-SP	Novus Biologicals	1:500
Lamin B (M-20)	sc-6217	Santa Cruz	1:200
Lamin B1 (B-10)	sc-374015	Santa Cruz	1:200
Lamin A (H-102)	sc-20680	Santa Cruz	1:200
Lamin A/C (E1)	sc-376248	Santa Cruz	1:200
Gamma-H2AX (Ser139)	80312	Cell Signaling	1:200
Gamma-H2AX (Ser139)	9718	Cell Signaling	1:200
HSP90 α/β (F-8)	sc-13119	Santa Cruz	1:200
Nesprin1-E	MANNES1E	Glen Morris	1:500
Nesprin-1-A	MANNES1A	Glen Morris	1:500
alpha-tubulin	T9026	Sigma	1:500(IF) 1:5000(WB)
NPC (414)	Ab50008	Abcam	1:500
Emerin	NCL-EMERIN	Leica	1:200
DNA-PKcs (S2056)	ab18192	Abcam	1:1000
DNA-PKcs	sc-390849	Santa Cruz	1:750
Cleaved Caspase-3	9661	Cell Signaling	1:500

Supplemental Table 1. Antibodies and corresponding dilutions. Primary antibodies for immunofluorescence staining and western blotting.